IL NUOVO CIMENTO Vol. 26 C, N. 3 Maggio-Giugno 2003

Development of a grid-dispersion model in a large-eddy-simulation–generated planetary boundary layer

U. Rizza([1]), G. Gioia([1])([2]), C. Mangia([1]) and G. P. Marra([1])([3])

([1]) *CNR, ISAC, Sezione di Lecce - Lecce, Italy*
([2]) *Dipartimento di Scienze dei Materiali, Università di Lecce - Lecce, Italy*
([3]) *Dipartimento di Ingegneria dell'Innovazione, Università di Lecce - Lecce, Italy*

(ricevuto il 29 Ottobre 2002; approvato l'11 Aprile 2003)

Summary. — Numerical simulations of dispersion experiments within the planetary boundary layer are actually feasible making use of Large Eddy Simulations (LES). In Eulerian framework, a conservation equation for a passive scalar may be superimposed on LES wind/turbulence fields to get a realistic description of time-varying concentration field. Aim of this work is to present a numerical technique to solve the Eulerian conservation equation. The technique is based on Fractional Step/Locally One-Dimensional (LOD) methods. Advection terms are calculated with a semi-Lagrangian cubic-spline technique, while diffusive terms are calculated with Crank-Nicholson implicit scheme. To test the grid model, the dispersion of contaminants emitted from an elevated continuous point source in a convective boundary layer is simulated. Results show that the calculated concentration distributions agree quite well with numerical and experimental data found in the literature.

PACS 92.60.Ek – Convection, turbulence, and diffusion.
PACS 92.60.Sz – Air quality and air pollution.

1. – Introduction

Large eddy simulation has become a well-established technique to study the 3D turbulent characteristics of Planetary Boundary Layer (PBL) [1]. The physical basis of LES is the separation of the flow into large-scale motions which contain most of energy and are dependent on the flow environment, and small-scale motions which are believed to be more universal in character. The proper distinction between flow scales is accomplished by applying to the Navier-Stokes equations a high-pass filter with a cut-off length Δ_f. This means that the small scales are parameterized, while the large ones are solved explicitly by computing numerically the filtered equations. It is clear that LES will provide excellent simulations when the cut-off length Δ_f is much smaller of the scale of Energy Containing Eddies (ECE) of the turbulence.

The velocity and turbulence fields provided by LES may be used to calculate the transport and dispersion of contaminants. In this way one would obtain, at the same

time, detailed dispersion data and complete information on meteorological and turbulent parameters. Several studies with LES for atmospheric dispersion have been reported in the literature and concern both Eulerian and Lagrangian dispersion simulation approaches [2-5]. Providing a detailed knowledge of turbulence fields, Lagrangian particle models are very successful in describing turbulent dispersion of passive contaminants because they are able to take into account essential aspects of turbulence, but they are limited to simplified set of reacting species. On the other side, Eulerian approach being based on conservation equation, can incorporate the numerous second- and high-order chemical kinetic equations necessary to describe photochemical smog generation, which represents, presently, a challenging problem. The critical point is the numerical scheme for the conservation equation which can generate nonphysical results.

Aim of this paper is to present a numerical technique to solve the Eulerian conservation equation using the gridded wind/turbulence field generated by Moeng's LES code [6]. The technique is based on Fractional Step/Locally One-Dimensional methods [7-9]. Advection terms are calculated with a semi-Lagrangian cubic-spline technique [10], while diffusive terms are calculated with Crank-Nicholson implicit scheme. To avoid unwanted numerical noises produced by the advection numerical scheme, a non-linear filter [11] is used. The main advantage of this scheme with respect to those ones involved in most used air pollution grid models [12], consists in its better adaptability to domains with irregular grid-spacing.

To test the grid model, the dispersion processes of passive contaminants emitted from an elevated source in a convective boundary layer are simulated. This represents the first step before to extend the technique to more complex cases and to reactive species. Simulation results are compared with laboratory data of Willis and Deardoff [13, 14].

2. – The large eddy model

The large eddy model used in this study is the same as described by Moeng [6] with the further developments described in [1, 15]. Here, we will only give a short outcome.

In the LES technique, the smallest eddies in a large Reynolds number PBL flow are removed by applying a spatial filter function to the Navier-Stokes equations [16]. For each turbulent quantity f, the filtered (or resolved) variable, denoted by an overbar, is defined as

$$\overline{f}(\mathbf{x},t) = \int_D f(\mathbf{y},t)\overline{G}(\mathbf{x}-\mathbf{y})\mathrm{d}y = \int_D f(\mathbf{x}-\mathbf{y},t)\overline{G}(\mathbf{y})\mathrm{d}\mathbf{y}\,. \tag{1}$$

Integration is over the flow volume D. The function $\overline{G}$ is a three-dimensional low-pass filter that removes the subgrid scale fluctuations (or small eddies: $f'(\mathbf{x},t)$).

Applying the filtering operator to the incompressible Navier-Stokes equations and making the substitution $f(\mathbf{x},t) = \overline{f}(\mathbf{x},t) + f'(\mathbf{x},t)$, we obtain the governing equations for the filtered variables:

$$\frac{\partial \overline{u_i}}{\partial t} + \frac{\partial \overline{\overline{u_i}\,\overline{u_j}}}{\partial x_j} = -\frac{1}{\rho}\frac{\partial \overline{p}}{\partial x_i} - \frac{\partial T_{ij}}{\partial x_j} + \nu\frac{\partial^2 \overline{u_i}}{\partial x_j \partial x_j} + g_i\frac{\theta}{\theta_0} - 2\varepsilon_{ijk}\Omega_j\overline{u_k}\,, \tag{2}$$

where $i \equiv (x, y, z)$, ρ is the density, $\overline{p}$ is the pressure term, $\nu = \mu/\rho$ is the kinematic viscosity, μ is the dynamic viscosity, the gravitational acceleration g_i is non-zero only in the z direction, θ is the virtual potential temperature, θ_0 is the temperature of some

reference state, ε_{ijk} is the permutation tensor and Ω_j is the angular vector of the earth's rotation. The terms

$$T_{ij} = \overline{u_i' \overline{u}_j} + \overline{\overline{u}_i u_j'} + \overline{u_i' u_j'} \tag{3}$$

are the subgrid scale fluxes which represent the effect of the subgrid scale on the resolved field.

The tensor T_{ij} is modeled following the Smagorinsky-Lilly hypothesis [17, 18]

$$T_{ij} = -K_M \left(\frac{\partial \overline{u}_i}{\partial x_j} + \frac{\partial \overline{u}_j}{\partial x_i} \right). \tag{4}$$

The eddy viscosity coefficient K_M is expressed as

$$K_M = C_k l(e^{1/2}), \tag{5}$$

where C_k is a diffusion coefficient to be determined, l is the mixing length and e is the subgrid turbulent energy.

For unstable stratification, l is related to the grid size $l = \Delta = (\Delta x \Delta y \Delta z)^{1/3}$, while for a stable temperature stratification, the length scale is related to the Brunt-Vaisala frequency [19]

$$l = 0.76 e^{1/2} \left(\frac{g}{\overline{\theta}_0} \frac{\partial \overline{\theta}}{\partial z} \right). \tag{6}$$

The SGS energy e is determined by the following prognostic equation:

$$\frac{\partial e}{\partial t} + \overline{u_i} \frac{\partial e}{\partial x_j} = P + B - \varepsilon + D, \tag{7}$$

where the different terms on the right-hand side are shear production P, buoyancy B, dissipation ε and diffusion D [1].

3. – Eulerian dispersion of a passive contaminant

The filtered conservation equation for a generic scalar C is given by

$$\frac{\partial \overline{C}}{\partial t} = -\frac{\partial \overline{u}_i \overline{C}}{\partial x_i} - \frac{\partial \tau_{ci}}{\partial x_i} + S_Q, \tag{8}$$

where $S_Q = Q\delta(x)\delta(y)\delta(z - H_S)$ is the source term, where Q is the rate emission, H_S is the source height, τ_{ci} are the SGS turbulent scalar fluxes. The closure model for τ_{ci} is

$$\tau_{ci} = -K_C \frac{\partial \overline{C}}{\partial x_i}, \tag{9}$$

where K_C is the eddy diffusivity for a scalar quantity. Introducing the SGS Schmidt number

$$S_c = \frac{K_M}{K_C}, \tag{10}$$

we can express the eddy diffusivity in terms of eddy viscosity:

$$\tau_{ci} = -\frac{K_M}{S_c}\frac{\partial \overline{C}}{\partial x_i}\,. \tag{11}$$

Substitution of eq. (11) into eq. (8) leads to

$$\frac{\partial \overline{C}}{\partial t} = -\frac{\partial \overline{u}_i \overline{C}}{\partial x_i} + \frac{1}{S_c}\frac{\partial}{\partial x_i}\left[K_M \frac{\partial \overline{C}}{\partial x_i}\right] + S_Q\,. \tag{12}$$

Following [20] we assumed $S_c = 0.33$.

The filtered wind components $\overline{u_i}$ and the SGS eddy diffusivity K_M in each grid point are provided by LES.

4. – Numerical method

Numerical solution of eq. (12) is not trivial because of numerical diffusion and consequent generation of non-physical results.

The numerical method consists in splitting eq. (12) into a set of time-dependent equations, each one Locally One-Dimensional (LOD) [7], [8] and [9]:

$$\frac{\partial \overline{C}}{\partial t} = \sum_{i=1}^{3} \Lambda_i \overline{C}\,, \tag{13}$$

where Λ_i is the sum of the advective and diffusive operators

$$\Lambda_i = A_i + D_i \equiv -\overline{u}_i \frac{\partial}{\partial x_i} + \frac{1}{S_c}\frac{\partial}{\partial x_i}\left(K_M \frac{\partial}{\partial x_i}\right)\,. \tag{14}$$

Using Crank-Nicholson time integration we have

$$\overline{C}^{\,n+1} = \prod_{j=1}^{3}\left[I - \frac{\Delta t}{2}\Lambda_j\right]^{-1}\left[I + \frac{\Delta t}{2}\Lambda_j\right]\overline{C}^{\,n} = \prod_{j=1}^{3} T_j^n \overline{C}^{\,n}\,, \tag{15}$$

where I is the unity matrix.

To obtain second-order accuracy, it is necessary to reverse the order of the operators at each alternate step to cancel the two non-commuting terms. Therefore, we replace the scheme (15) with the following double-sequence equations:

$$\overline{C}^{\,n} = \prod_{j=1}^{3} T_j^n \overline{C}^{\,n-1}\,, \tag{16a}$$

$$\overline{C}^{\,n+1} = \prod_{j=3}^{1} T_j^n \overline{C}^{\,n}\,. \tag{16b}$$

In order to develop a scheme that preserves peaks, retain positive quantities, and does not severely diffuse sharp gradients, after each advective step a filtering procedure

is applied. This is necessary for damping out the small-scale perturbations before they can corrupt the basic solution.

So, the effective system utilized is the following:

$$\overline{C}^{\,n} = \prod_{i=1}^{3} [A_i F D_i]\, \overline{C}^{\,n-1}\,, \tag{17}$$

$$\overline{C}^{\,n+1} = \prod_{i=1}^{3} [D_i A_i F]\, \overline{C}^{\,n}\,, \tag{18}$$

where the operator F represents the filter operation described in [11].

The advective terms (operators A_i), which are usually the most difficult to implement, are solved using a method based on cubic-spline interpolations, while a Crank-Nicholson implicit scheme is used for the diffusive terms (operators D_i).

4˙1. *Details of the fractional step/locally one-dimensional method.* – The finite difference algorithm for eq. (17) (or its reverse eq. (18)) contains three steps, one for each direction. In the following we only show the numerical scheme for the x direction, the scheme being the same for the other directions with the appropriate boundary conditions.

We use the notation $j \in [1, N_x], k \in [1, N_y], m \in [1, N_z]$ for increments in the (x, y, z) Cartesian space, so we have

$$\begin{aligned} x_j &= x_0 + j\Delta x\,, \\ y_k &= y_0 + k\Delta y\,, \\ z_m &= z_0 + m\Delta z\,, \end{aligned}$$

where Δx, Δy, Δz are the grid sizes and (N_x, N_y, N_z) are the number of grid points along the x, y, z directions, respectively.

For each direction, the scheme (eqs. (17) and (18)) contains three sub-steps: a) the advective part, b) the filtering procedure, c) the diffusive part.

a) The advection is computed using a quasi-Lagrangian cubic-splines method [10,21], so for the operator A_x we have

$$\overline{C}^{\,h+\frac{1}{2}}_{j,k,m} = S^h(x_j - \alpha\Delta x)\,, \qquad \text{if} \quad \overline{u}^{\,h}_{j,k,m} \geqslant 0\,, \tag{19}$$

$$\overline{C}^{\,h+\frac{1}{2}}_{j,k,m} = S^h(x_j + \alpha\Delta x)\,, \qquad \text{if} \quad \overline{u}^{\,h}_{j,k,m} < 0\,, \tag{20}$$

with $\alpha = \overline{u}^{\,h}_{j,k,m} \frac{\Delta t}{\Delta x}$, the superscript h denotes an intermediate fictitious time step between n and $n+1$. This is called Fractional Steps (FS) technique.

The interpolation function (cubic-spline) S may be expressed in terms of the spline derivatives $P^h_j = \left(\frac{\partial \overline{C}}{\partial x}\right)^h_{j,k,m}$ as

$$\begin{aligned} S^h(x) = {} & P^h_{j-1} \frac{(x_j - x)^2 (x - x_{j-1})}{h_j^2} - P^h_j \frac{(x - x_{j-1})^2 (x_j - x)}{h_j^2} + \\ & + \overline{C}^{\,h}_{j-1} \frac{(x_j - x)^2 [2(x - x_{j-1}) + h_j]}{h_j^3} + \overline{C}^{\,h}_j \frac{(x - x_{j-1})^2 [2(x_j - x) + h_j]}{h_j^3}\,, \end{aligned} \tag{21}$$

where $h_j = x_j - x_{j-1}$ [22].

The spline derivatives are obtained by solving the tridiagonal algebric system [22,23]:

$$\frac{1}{2}P^h_{j-1} + 2P^h_j + \frac{1}{2}P^h_{j+1} = \frac{3}{2\Delta x}\left(\overline{C}^h_j - \overline{C}^h_{j-1}\right) + \frac{3}{2\Delta x}\left(\overline{C}^h_{j+1} - \overline{C}^h_j\right) . \tag{22}$$

Using eqs. (21), (22), eqs. (19), (20) become, respectively,

$$\begin{aligned}\overline{C}^{h+\frac{1}{2}}_{j,k,m} = {} & \overline{C}^h_{j,k,m} - P^h_j h_j \alpha + \\ & + \left[P^h_{j-1}h_j + 2P^h_j h_j + 3\left(\overline{C}^h_{j-1,k,m} - \overline{C}^h_{j,k,m}\right)\right]\alpha^2 - \\ & - \left[P^h_{j-1}h_j + P^h_j h_j + 2\left(\overline{C}^h_{j-1,k,m} - \overline{C}^h_{j,k,m}\right)\right]\alpha^3 ,\end{aligned} \tag{23a}$$

$$\begin{aligned}\overline{C}^{h+\frac{1}{2}}_{j,k,m} = {} & \overline{C}^h_{j,k,m} + P^h_j h_{j+1} \alpha - \\ & - \left[P^h_{j+1}h_{j+1} + 2P^h_j h_{j+1} + 3\left(\overline{C}^h_{j,k,m} - \overline{C}^h_{j+1,k,m}\right)\right]\alpha^2 + \\ & + \left[P^h_j h_{j+1} + P^h_{j+1}h_{j+1} + 2\left(\overline{C}^h_{j,k,m} - \overline{C}^h_{j+1,k,m}\right)\right]\alpha^3 .\end{aligned} \tag{23b}$$

b) After each advective step, a filter operation is applied to the intermediate field to remove any negative concentration which is usually produced by the advection

$$\overline{C}^{h+\frac{1}{2}}_{j,k,m} = F\left(\overline{C}^{h+\frac{1}{2}}_{j,k,m}\right) .$$

c) Finally, the diffusive step (operator D_x) is computed by means of Crank-Nicholson implicit scheme

$$\begin{aligned}\frac{\overline{C}^{h+1}_{j,k,m} - \overline{C}^{h+\frac{1}{2}}_{j,k,m}}{\Delta t} = {} & \frac{1}{2S_c}\left[\frac{K'_M\left(\overline{C}^{h+\frac{1}{2}}_{j+1,k,m} - \overline{C}^{h+\frac{1}{2}}_{j,k,m}\right) - K''_M\left(\overline{C}^{h+\frac{1}{2}}_{j,k,m} - \overline{C}^{h+\frac{1}{2}}_{j-1,k,m}\right)}{(\Delta x)^2}\right] + \\ & + \frac{1}{2S_c}\left[\frac{K'_M\left(\overline{C}^{h+1}_{j+1,k,m} - \overline{C}^{h+1}_{j,k,m}\right) - K''_M\left(\overline{C}^{h+1}_{j,k,m} - \overline{C}^{h+1}_{j-1,k,m}\right)}{(\Delta x)^2}\right] ,\end{aligned} \tag{24}$$

where $K'_M = K_M(x_{j+1/2})$, $K''_M = K_M(x_{j-1/2})$.

4˙2. *Boundary conditions.* – Equations (23a), (23b) and (24) are the numerical schemes for advective/diffusive terms in x direction. As we said, similar schemes are obtained for y and z directions with the appropriate boundary conditions.

Boundary conditions for the advective terms

We assume, for every time step, zero gradient boundary conditions and zero outflow

boundary conditions, *i.e.*

$$\text{for } j = 1 : \quad \begin{cases} P_0^h = 0\,, \\ \overline{C}_{0,k,m}^h = 0\,; \end{cases} \tag{25a}$$

$$\text{for } j = N_x : \quad \begin{cases} P_{N_x}^h = 0\,, \\ \overline{C}_{N_x+1,k,m}^h = 0\,. \end{cases} \tag{25b}$$

Analogous conditions are applied along y and z directions.

Boundary conditions for the diffusion terms

We assumed, for every time step, the zero outflow boundary conditions, *i.e.*

$$\text{for } j = 1 : \quad \overline{C}_{0,k,m}^{h+1} = \overline{C}_{0,k,m}^{h+\frac{1}{2}} = 0\,, \tag{26a}$$

$$\text{for } j = N_x : \quad \overline{C}_{N_x+1,k,m}^{h+1} = \overline{C}_{N_x+1,k,m}^{h+\frac{1}{2}} = 0\,. \tag{26b}$$

Analogous conditions are applied along y direction.

For diffusion along z direction, the boundary conditions are the zero gradient conditions, that is

$$\text{for } m = 1 : \quad \overline{C}_{j,k,0}^h = \overline{C}_{j,k,1}^h\,, \tag{27a}$$

$$\text{for } m = N_z : \quad \overline{C}_{j,k,N_z+1}^h = \overline{C}_{j,k,N_z}^h\,. \tag{27b}$$

5. – Simulations

In order to test the grid model described, a dispersion experiment in a convective turbulent regime is simulated. The procedure is the following. First we run the large eddy model for a sufficient time period to reach a quasi-stationary turbulence field, then we inject a contaminant into the numerical domain and integrate simultaneously the large eddy model and the conservation equation.

5˙1. *Experiment characteristics.* – It is well known that turbulence within the PBL is generated by two main forcing mechanisms: mechanical and convective. The former is related to wind shear, and is governed by geostrophic wind. The latter is directly related to the surface heat flux and it is generally responsible for convective transport of momentum, heat and any other scalar.

Our simulation concerns a convective PBL. The calculations are performed in a rectangular domain arranged in a way that it could comprise several updrafts at a given time. The dimensions of the box are 10×10 km in the horizontal directions and 2 km in the vertical direction.

The resolution is 128 grid points in x and y directions, 96 grid points in z direction. The simulation started from a laminar flow, with the geostrophic wind constant throughout the whole numerical domain. Turbulence is generated by heating the surface at a constant rate. External parameters—extension of domain , grid size, geostrophic winds, surface heat flux, initial capping inversion height—are summarised in table I. Time step is set equal to 2 seconds. After some time a layer with quasi-stationary convective turbulence establishes itself. This condition is obtained after the LES run for 5000 time

TABLE I. – *External simulation parameters.*

Mesh grid points	Domain size	Geostrophic wind	Surface heat flux	Initial inversion height
(N_x, N_y, N_z)	L_x, L_y, L_z (km)	(U_g, V_g) (m/s)	Q_* ($\mathrm{ms}^{-1}\mathrm{K}$)	$(z_i)_0$ (m)
(128,128,96)	(10,10,2)	(10,0)	0.24	1000

steps (more than two hours of real simulated time). This represents our initial conditions ($t = 0$) for dispersion experiment. The micrometeorological parameters are indicated in table II.

At $t = 0$, a contaminant is injected from an elevated point source placed at half height of the boundary layer height ($H_S = H_{\mathrm{mix}}/2$) into the box domain. The contaminant is introduced every two time steps to satisfy the double sequence scheme (eqs. ($16a$), ($16b$)). After the initial time, we continue the integration of the large eddy model which is subjected to the same heating rate. The evolution of the point source is calculated simultaneously by solving the conservation equation for the scalar.

5˙2. *Test of the advection-algorithm.* – It is well known that any numerical scheme which calculates the concentration should satisfy the following requirements [2]:

1) conservation of mass;

2) positive definiteness;

3) maintenance of sharp gradients.

The importance of the first two requirements is clear. In fact, it is fundamental for any dispersion simulation that the mass of contaminant should keep a constant value during the simulation in order to satisfy conservation principles. Moreover, since the concentration is a positive definite variable it is clear that its value cannot go below zero. Concerning the third point, since during the initial phase of a plume/puff dispersion the instantaneous concentration fields are characterized by sharp concentration gradients, each simulation of plumes or puffs has to maintain such gradients. This is, in general, difficult to obtain, because the initial resolution is often inadequate. Moreover, it is well known that any advection scheme may suffers from severe phase errors, which displace the computed concentration peaks from their true locations, and/or artificial diffusion, which smears out the concentration peaks [24].

To test the algorithm capability to satisfy the three requirements, we advected a cube of passive contaminant by a constant wind only along x direction [10].

In particular, to assess the conservation of mass we used the mass conservation ratio [24], *mcr*, which is the ratio between the total mass in a generic instant and the initial

TABLE II. – *Internal simulation parameters. ustar is the friction velocity, wstar is the free convective velocity and* L_{MO} *is the Monin-Obukhov length.*

ustar (m/s)	wstar (m/s)	$H_{\mathrm{mix}}/L_{\mathrm{MO}}$	H_{mix} (m)
0.7	2.1	-18	1100

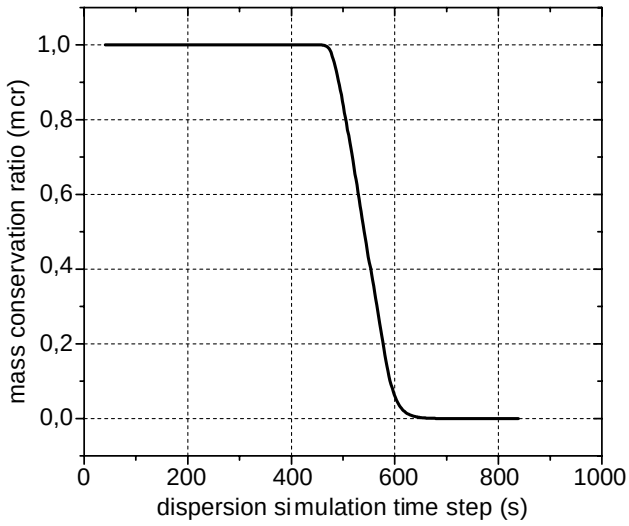

Fig. 1. – Mass conservation ratio during the dispersion simulation.

mass

$$mcr = \sum_{j,k,i} \overline{C}_{j,k,i}\,(t) \Big/ \sum_{j,k,i} \overline{C}_{j,k,i}\,(0)\ . \tag{28}$$

The result of the advection test is showed in fig. 1. It is evident that the numerical scheme conserves mass with high precision: the *mcr* keeps unit value until the contaminant is inside the box domain, it decreases when the contaminant crosses the boundary.

Figures 2a and 2b show the crosswind concentration distribution before and after the the application of the filter. It can be seen that the filtering procedure assures the positive definiteness of the concentration field.

The third requirement, *i.e.* the maintenance of sharp gradients, is strictly related to the concentration distribution. In table III the (x, z)-locations of crosswind-integrated peak concentration are summarised: it is evident as during the advection the variation of maximum concentration is around 10% with respect to the maximum value.

Based on the test results, we conclude that the implemented numerical scheme works quite satisfactory.

TABLE III. – *Location and intensity of concentration peaks during advection.*

X (m)	Z (m)	C_{peak} (μg/m^3)
1927	187.5	2325
3490	187.5	2603
4948	187.5	2508

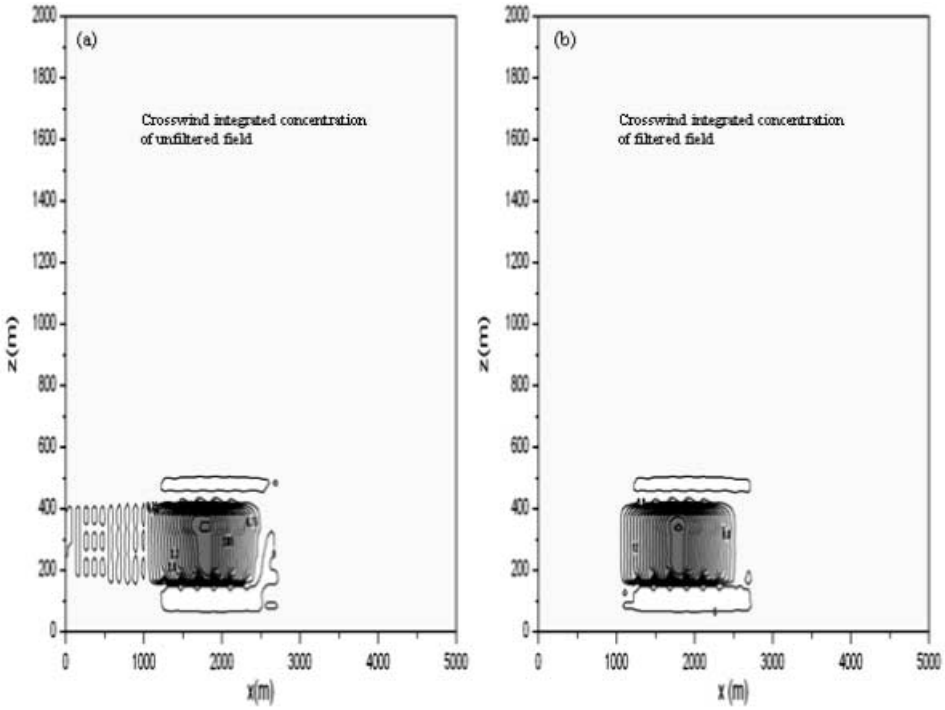

Fig. 2. – Concentration distribution before the filtering application (a) and after (b).

5˙3. *Dispersion simulation and results*. – The main characteristics of passive plume dispersion in the CBL have been demonstrated through numerical predictions [25-27], field observations [28, 29], and in a more detailed way through laboratory experiments of [13] and [14] in late 70s. All these studies showed that in the CBL, the plume centreline, defined as the locus of maximum concentration, from an elevated source descends until it reaches the ground, it remains there for some distance and then it rises. The descent of the plume centreline is due to the size, long life, and organized nature of the downdrafts characteristics of the CBL. Because of the greater areal coverage of downdrafts the probability of material to be released into them is higher.

In our experiment, the contaminant is injected from an elevated point, located at $H_S = H_{\mathrm{mix}}/2$, all along the duration of simulation (release time = 5000 time steps) each two time steps. The travel time, which is a rough estimate of how long the plume takes to cross the longitudinal domain (10 km), is about 200 time steps. To get a proper plume behaviour of PBL dispersion, sampling and release time should be greater than travel time. In order to satisfy this constrain, we choose a concentration averaging time of 4000 time steps.

Let us introduce the crosswind–integrated concentration by

$$C_y = \frac{1}{\Delta T} \int\limits_{\Delta T} \int\limits_{L_y} \overline{C}\,(x, y, z)\,\mathrm{d}y\mathrm{d}t\,,$$

ΔT is an arbitrary average interval. This concentration is made dimensionless by dividing

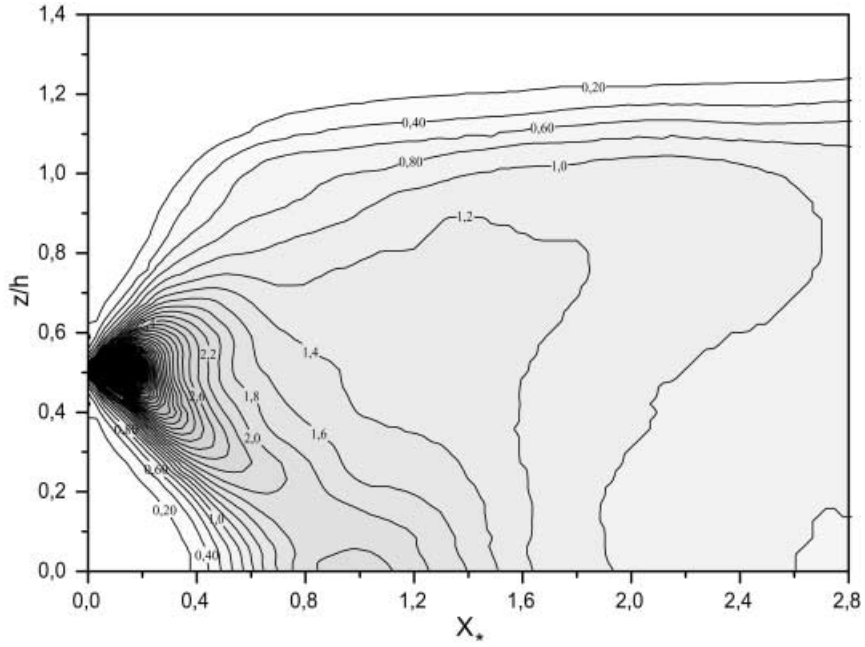

Fig. 3. – Crosswind-integrated concentration averaged between last 3000 time steps, as a function of dimensionless height and downwind distance.

by Q/UH_{mix}, where U is the mean longitudinal wind velocity. Figure 3 shows the adimensional crosswind-integrated concentration *vs.* the non-dimensional distance X_*, defined by $\frac{x/U}{H_{\mathrm{mix}}/w_*}$.

Figure 4 shows the ground-level concentration *vs.* the adimensional distance compared with Willis and Deardoff [13, 14] data.

It is evident by the figures that dispersion model reproduces the main characteristics of the plume dispersion. The greatest concentration is found along a descending path from the source. There is a good agreement both for the value and the position of maximum concentration.

6. – Conclusions

Large Eddy Simulation represents nowadays a very powerful method in calculating 3D turbulent structures which are fundamental for describing any dispersion phenomena in the planetary boundary layer.

In this work we utilised LES for modelling Eulerian dispersion of passive contaminants as first step before to extend it to reactive species. To solve numerically the conservation equation we utilised a splitting technique developed in 70s by Soviet mathematicians. The advective terms which present, from a numerical point of view, many difficulties in their discretisation are solved with a quasi-Lagrangian cubic-spline technique. Such scheme has been preferred as it can be easily adapted to domains with irregular grid-spacing [21].

To test the model, we have simulated dispersion of an elevated continuous point source in a convective boundary layer. The non-trivial characteristics of dispersion are

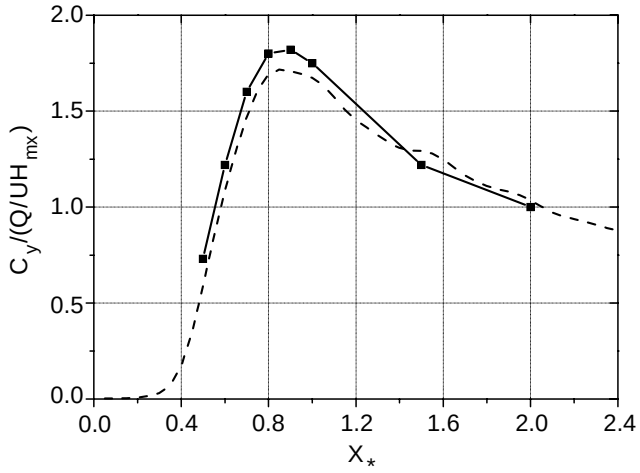

Fig. 4. – Crosswind-integrated surface concentration as a function of dimensionless downwind distance. The dashed line represents our simulation result, the solid line represents Willis and Deardorff experimental data.

adequately captured and the crosswind-integrated concentration distribution resembles closely the well-established numerical and laboratory experiments found in the literature. Results confirm that LES constitutes an alternative for field experiments: it can provide databases of dispersion data on which a wide range of dispersion models can be developed and tested, in view of their utilisation for air quality applications.

* * *

We thanks Mr. C. Elefante for his technical support.

REFERENCES

[1] Sullivan P. P., Mc Williams J. C. and Moeng C. H., *Boundary-Layer Meteorol.*, **71** (1994) 247.
[2] Nieuwstadt F. T. M. and De Valk J. P. J. M. M., *Atmos. Environ.*, **21** (1987) 2573.
[3] Van Haren L. and Nieuwstadt F. T. M., *J. Appl. Meteorol.*, **28** (1989) 818.
[4] Meeder J. P. and Nieuwstadt F. T. M., *Atmos. Environ.*, **34** (2000) 3563.
[5] Kemp J. R. and Thompson D. J., *Atmos. Environ.*, **30** (1996) 2911.
[6] Moeng C. H., *J. Atm. Sci.*, **41** (1984) 2052.
[7] Yanenko N. N., in *The Method of Fractional Steps* (Springer-Verlag, Berlin, New York) 1971, pp. 27-33.
[8] Mc Rae G. J., Goodin W.r. and Seifeld J. H., *J. Comp. Phys.*, **45** (1982) 1.
[9] Marcuk N. N., in *Metodi del Calcolo Numerico* (Editori Riuniti, Roma) 1984, pp. 245-289.
[10] Pielke R. A., in *Mesoscale Meteorological Modeling* (Academic Press, San Diego-CA) 1984, pp. 272-307.
[11] Forester C. K., *J. Comp. Phys.*, **23** (1979) 1.
[12] Yamartino R. J. and Scire Y. S., *Atmos. Environ.*, **26** (1992) 1493.
[13] Willis G. E. and Deardorff J. W., *Q. J. R. Meteorol. Soc.*, **102** (1976) 427.
[14] Willis G. E. and Deardorff J. W., *Atmos. Environ.*, **15** (1981) 109.
[15] Moeng C. H. and Sullivan P. P., *J. Atm. Sci.*, **51** (1994) 999.

[16] Leonard A., *Adv. Geophys. A*, **18** (1974) 237.
[17] Lilly D. K., Technical Report No. 123, NCAR, Boulder, CO (1966).
[18] Smagorinsky J., *Mon. Weather Rev.*, **91** (1963) 99.
[19] Deardorff J. W.,, *Boundary-Layer Meteorol.*, **18** (1980) 495.
[20] Andren A., Brown A. R.,Graf J., Mason P. J., Moeng C. H., Nieuwstadt F. T. M. and Schumann U., *Q. J. R. Meteorol. Soc.*, **120** (1994) 1457.
[21] Long P. E. and Pepper D. W., *J. Appl. Meteorol.*, **20** (1981) 146.
[22] Ahlberg J. H., Nilson E. N., Walsh J. L.,in *The Theory of Splines and their Applications* (Academic Press, New York) 1967.
[23] Price G. V. and Mac Pherson A. K., *J. Appl. Meteorol.*, **12** (1973) 1102.
[24] Chock D. P. and Dunker A. H., *Atmos. Environ.*, **17** (1983) 11.
[25] Lamb R. G., *Atmos. Environ.*, **12** (1978) 1297.
[26] Lamb R. G., *The effects of release height on material dispersion in the convective boundary layer*, in 4^{th} *Symposium on Turbulence, Diffusion and Air Pollution* (Amer. Meteorol. Soc., Boston) 1979, pp. 27-33.
[27] Lamb R. G., *J. Appl. Meteorol.*, **20** (1982) 391.
[28] Nieuwstadt F. T. M., *J. Appl. Meteorol.*, **19** (1980) 157.
[29] Moninger W. R., Eberhard W. L., Briggs G. A., Kropfli R. A. and Kaimal J. C., *Simultaneous radar and lidar observations of plumes from continuous point sources*, in 21^{st} *Conference on Radar Meteorology* (Amer. Meteorol. Soc., Boston) 1983, pp. 246-250.